

# Secure Dual-functional Radar-Communication Transmission: Hardware-Efficient Design

(Invited Paper)

Nanchi Su<sup>1</sup>, Fan Liu<sup>2</sup>, Christos Masouros<sup>1</sup>, Tharmalingam Ratnarajah<sup>3</sup>, and Athina Petropulu<sup>4</sup>

<sup>1</sup> Department of Electronic and Electrical Engineering, University College London, London, UK

<sup>2</sup> Department of Electrical and Electronic Engineering, Southern University of Science and Technology, Shenzhen, China

<sup>3</sup> Institute for Digital Communications, School of Engineering, University of Edinburgh, Edinburgh, UK

<sup>4</sup> Department of Electrical and Computer Engineering Rutgers, State University of New Jersey, Piscataway, NJ USA

**Abstract**—This paper investigates the constructive interference (CI) based constant envelope (CE) waveform design problem aiming at enhancing the physical layer (PHY) security in dual-functional radar-communication (DFRC) systems. DFRC systems detect the radar target and communicate with downlink cellular users in wireless networks simultaneously, where the radar target is regarded as a potential eavesdropper which might surveil the data from the base station (BS) to communication users (CUs). The CE waveform and receive beamforming are jointly designed to maximize the signal to interference and noise ratio (SINR) of the radar under the security and system power constraints when the target location is imperfectly known. The optimal solution is obtained by the max-min fractional programming (FP) method. Specifically, the problem is designed to maximize the minimum SINR of the radar in the target location angular interval. Simulation results reveal the effectiveness and the hardware efficiency of the proposed algorithm.

**Index Terms**—Dual-functional radar-communication, physical layer security, constant envelope, constructive interference

## I. INTRODUCTION

The spectrum source is getting increasingly congested due to the tremendous growth of wireless connections and mobile devices, which motivates the development of dual-functional radar-communication (DFRC) systems in recent years. In DFRC systems, the transmitted waveform is specifically designed as to serve for both purposes of target sensing and wireless communication, which raises unique security challenges. Intuitively, the radar beampattern is designed to concentrate the radiation power towards the direction of targets of interest so as to improve the detection performance. Since the probing DFRC signal also carries information for the communication users, the target, as a potential eavesdropper, e.g., an unauthorized vehicle or UAV, could readily surveil the information intended for communication users (CUs). To this end, new physical layer (PHY) security solutions are required for the dual functional operation in security-critical DFRC designs.

With respect to the security design, recent studies focus on exploiting constructive interference (CI) through symbol-level precoding, which exploits known multiuser interference (MUI) as useful power by pushing the received signal away from the detection bound of the signal constellation. Also, it

is provable that CI-based precoding designs benefit the data secrecy. In particular, the CI and artificial noise (AN) can be jointly exploited to design secure beamformer under the assumption of perfect or imperfect CSI [1], [2], which was proved to outperform the conventional AN-aided secrecy optimization. In addition to increasing the secrecy, the generated AN was exploited to be constructive to energy harvesting in [1]. Furthermore, the work of [3] expanded the scenario to more practical cases where the channel state information (CSI) of eavesdropper is totally unknown. In [4], practical transmitter designs were exploited when the CUs' channel is correlated with or without the eavesdropper's channel. We note that while all the above approaches are designed for the classical PHY security scenario involving legitimate users and external eavesdroppers, none of these apply to the unique DFRC scenarios where the target of interest may be a potential eavesdropper.

To address DFRC security in broader scenarios, it is worth studying the CI based waveform design for the reason that a) MUI is commonly treated as a detrimental impact that needs to be mitigated, while it becomes beneficial and further contributes to the useful signal power in CI design; b) CI based precoding can support a larger number of data streams with a significantly improved SER performance [5]. Moreover, motivated by the demand of power-efficient and cost-effective in multi-input multi-output (MIMO) systems, we deploy constant envelope (CE) waveform design in our problem formulations, which restricts the equivalent complex baseband signal at each antenna to have constant amplitude [6]. In practice, digital phase shifters (PSs) are mostly deployed, which provide a discrete set of phase states which are controlled by a string of binary digits [7].

In this paper, the CI technique is investigated to enhance the PHY layer security. Specifically, we consider a DFRC BS which serves CUs while detecting a point-like target in the presence of clutter, where the target is treated as a potential eavesdropper which might intercept the information intended to CUs. MUI is designed to be constructive at the CUs, while disrupting the data at the radar target, which deteriorates the target receive signals and thus increases the SER at the

target. Meanwhile, discrete phase CE and 1-bit digital-to-analog converters (DACs) constraints are taken into account for hardware cost reduction.

## II. SYSTEM MODEL

We consider a DFRC MIMO system with a BS equipped with  $N_T$  transmit antennas and  $N_R$  receive antennas, which is serving  $K$  single-antenna users and detecting a point-like target simultaneously. The target can be regarded as a potential eavesdropper which might intercept the information sent from the BS to legitimate users. Due to the existence of  $I$  clutter sources, the target return is interfered at the BS's receiver. Additionally, the communication channel is considered to be a narrowband slow time-varying block fading Rician fading channel. Based on the assumptions above, below we elaborate on the radar and communication signal models.

### A. Radar Signal Model

Let  $\mathbf{x} \in \mathbb{C}^{N_T \times 1}$  denote the transmit signal vector, the received waveform at the target is given as

$$\mathbf{r} = \underbrace{\alpha_0 \mathbf{U}(\theta_0) \mathbf{x}}_{\text{signal}} + \underbrace{\sum_{i=1}^I \alpha_i \mathbf{U}(\theta_i) \mathbf{x}}_{\text{signal-dependent clutter}} + \underbrace{\mathbf{z}}_{\text{noise}}, \quad (1)$$

where  $\alpha_0$  and  $\alpha_i$  denote the complex amplitudes of the target and the  $i$ -th interference source,  $\theta_0$  and  $\theta_i$  are the angle of the target and the  $i$ -th signal-dependent clutter source, respectively, and  $\mathbf{z} \in \mathbb{C}^{N_R \times 1}$  is the additive white Gaussian noise (AWGN) vector, with the variance of  $\sigma_R^2$ .  $\mathbf{U}(\theta)$  is the steering matrix of uniform linear array (ULA) antenna with half-wavelength spaced element, defined as

$$\mathbf{U}(\theta) = \mathbf{a}_r(\theta) \mathbf{a}_t^T(\theta), \quad (2)$$

where  $\mathbf{a}_t(\theta) = \frac{1}{\sqrt{N_T}} [1, e^{-j\pi \sin \theta}, \dots, e^{-j\pi(N_T-1) \sin \theta}]^T$  and  $\mathbf{a}_r(\theta) = \frac{1}{\sqrt{N_R}} [1, e^{-j\pi \sin \theta}, \dots, e^{-j\pi(N_R-1) \sin \theta}]^T$ . Then, the output of the filter can be given as

$$\begin{aligned} r_f &= \mathbf{w}^H \mathbf{r} \\ &= \alpha_0 \mathbf{w}^H \mathbf{U}(\theta_0) \mathbf{x} + \sum_{i=1}^I \alpha_i \mathbf{w}^H \mathbf{U}(\theta_i) \mathbf{x} + \mathbf{w}^H \mathbf{z}, \end{aligned} \quad (3)$$

where  $\mathbf{w} \in \mathbb{C}^{N_R \times 1}$  denotes the receive beamforming vector. Accordingly, the output SINR can be expressed as

$$\begin{aligned} \text{SINR}_{rad} &= \frac{|\alpha_0 \mathbf{w}^H \mathbf{U}(\theta_0) \mathbf{x}|^2}{\mathbf{w}^H \sum_{i=1}^I |\alpha_i|^2 \mathbf{U}(\theta_i) \mathbf{x} \mathbf{x}^H \mathbf{U}^H(\theta_i) \mathbf{w} + \mathbf{w}^H \mathbf{w} \sigma_R^2} \\ &= \frac{\mu |\mathbf{w}^H \mathbf{U}(\theta_0) \mathbf{x}|^2}{\mathbf{w}^H (\boldsymbol{\Sigma}(\mathbf{x}) + \mathbf{I}_{N_R}) \mathbf{w}}, \end{aligned} \quad (4)$$

where  $\mu = |\alpha_0|^2 / \sigma_R^2$ ,  $\boldsymbol{\Sigma}(\mathbf{x}) = \sum_{i=1}^I b_i \mathbf{U}(\theta_i) \mathbf{x} \mathbf{x}^H \mathbf{U}^H(\theta_i)$ , and  $b_i = |\alpha_i|^2 / \sigma_R^2$ .

Since  $\mathbf{x}$  is the intended information signal, the received signal at target (eavesdropper's receiver) can be given as

$$y_R = \alpha_0 \mathbf{a}_t^H(\theta_0) \mathbf{x} + e, \quad (5)$$

where  $e \sim \mathcal{CN}(0, \sigma_T^2)$  denotes the AWGN. Then, eavesdropping SNR at radar target can be expressed as

$$\text{SNR}_T = \frac{|\alpha_0 \mathbf{a}_t^H(\theta_0) \mathbf{x}|^2}{\sigma_T^2}. \quad (6)$$

### B. Communication Signal Model

The received signal at the  $k$ -th CU can be written as

$$y_k = \mathbf{h}_k^H \mathbf{x} + n_k, \quad (7)$$

where  $\mathbf{h}_k \in \mathbb{C}^{N_T \times 1}$  denotes the multiple-input-single-output (MISO) channel vector between the BS and the  $k$ -th CU. Similarly,  $n_k$  is the AWGN of the CU  $k$  with the variance of  $\sigma_{C_k}^2$ . We assume that  $\mathbf{h}_k$  is a slow time-varying block Rician fading channel, i.e., the channel is constant in a block but varies slowly from one block to another. Thus, the channel vector of the  $k$ -th user can be expressed as a combination of a deterministic strongest line-of-sight (LoS) channel vector and a multiple-path scattered channel vector, which is expressed as

$$\mathbf{h}_k = \sqrt{\frac{v_k}{1+v_k}} \mathbf{h}_{L,k}^{\text{LoS}} + \sqrt{\frac{1}{1+v_k}} \mathbf{h}_{S,k}^{\text{NLoS}}, \quad (8)$$

where  $v_k > 0$  is the Rician  $K$ -factor of the  $k$ -th user,  $\mathbf{h}_{L,k}^{\text{LoS}} = \sqrt{N_T} \mathbf{a}_t(\omega_{k,0})$  is the LoS deterministic component.  $\mathbf{a}(\omega_{k,0})$  denotes the array steering vector, where  $\omega_{k,0} \in [-\frac{\pi}{2}, \frac{\pi}{2}]$  is the angle of departure (AOD) of the LoS component from the BS to user  $k$  [8], [9]. The scattering component  $\mathbf{h}_{S,k}^{\text{NLoS}}$  can be expressed as  $\mathbf{h}_{S,k}^{\text{NLoS}} = \sqrt{\frac{N_T}{L}} \sum_{l=1}^L c_{k,l} \mathbf{a}_t(\omega_{k,l})$ , where  $L$  denotes the number of propagation paths,  $c_{k,l} \sim \mathcal{CN}(0, 1)$  is the complex path gain and  $\omega_{k,l} \in [-\frac{\pi}{2}, \frac{\pi}{2}]$  is the AOD associated to the  $(k, l)$ -th propagation path.

Then, we address the SNR expression at each CU when deploying CI technique, which has been widely investigated in the recent work [10]. Since CI-based waveform design aims to transform the undesirable MUI into useful power by pushing the received signal further away from the  $M$ -PSK decision boundaries, all interference contributes to the useful received power [11]. Herewith, the SNR of the  $k$ -th user is expressed as

$$\text{SNR}_k = \frac{|\mathbf{h}_k^H \mathbf{x}|^2}{\sigma_{C_k}^2}. \quad (9)$$

Additionally, we note that the intended symbol varies at a symbol-by-symbol basis in CI precoding designs. Let  $s_k$  denote the intended symbol of the  $k$ -th CU, which is  $M$ -PSK modulated. To this end, we define  $s_k \in \mathcal{A}_M$ , where  $\mathcal{A}_M = \{a_m = e^{j(2m-1)\phi}, m = 1, \dots, M\}$ ,  $\phi = \pi/M$ , and  $M$  denotes the modulation order.

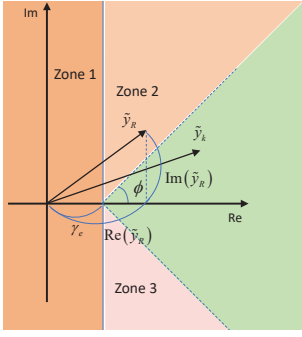


Fig. 1. The constructive and destructive region division for QPSK.

### III. CI PRECODING WITH DESTRUCTIVE INTERFERENCE TO THE RADAR RECEIVER

In this section, we consider the information transmission security of the DFRC system with the knowledge of precise target location. We assume that the communication users are legitimate, and treat the point-like target as a potential eavesdropper which might surveille the information from BS to CUs. Accordingly, in the following design, we aim to maximize the SINR at radar receiver, while confining the received signal at the target into the destructive region of the constellation, in order to ensure the PHY security for DFRC transmission.

#### A. Security Design with 1-bit DACs

In prior work with respect to DM technique, such as algorithms proposed in [12], the problems are designed based on the CSI of legitimate users, where the symbols received by potential eavesdroppers are scrambled due to the channel disparity. However, PHY security cannot be explicitly guaranteed in this way. To be specific, Taking QPSK modulation as an example, the intended symbol can be intercepted with a  $\frac{1}{4}$  probability at the target when the target's channel is independent with the CUs' channels, while more importantly, the probability of the target intercepting increases when the target and CUs' channels are correlated.

While the CI-based precoding guarantees low SER at CUs, we still need to focus on the detection performance at the target in order to prevent the transmit information from being decoded. Thus, the following problem is designed to improve the SER at the target. In detail, we define the region out of the constructive region as destructive region. As illustrated in Fig. 1, we design the CI-based precoding optimization problem aiming at restricting the received signals of CUs and the potential eavesdropper in the constructive and destructive area, respectively.

With the knowledge of the channel information, all CUs' data, as well as the location of target and clutter resources is readily available at the transmitter, the received signals at CUs can be constrained in the constructive region by

$$|\arg(\tilde{\mathbf{h}}_k^H \mathbf{x}) - \arg(s_k)| \leq \xi, \forall k, \quad (10a)$$

$$\text{SNR}_k \geq \Gamma_k, \forall k, \quad (10b)$$

where  $\Gamma_k$  is the given SNR threshold, and  $\xi$  is the phase threshold where the noise-less received symbols are supposed to lie. According the problem formulation proposed in [10], the constraints (10c) and (10d) can be recast as

$$|\text{Im}(\tilde{\mathbf{h}}_k^H \mathbf{x})| \leq \left( \text{Re}(\tilde{\mathbf{h}}_k^H \mathbf{x}) - \sqrt{\sigma_{C_k}^2 \Gamma_k} \right) \tan \phi, \forall k. \quad (11)$$

Regarding the received signal at the target, we can likewise give the expression of the destructive region as

$$|\text{Im}(\tilde{y}_R)| \geq \left( \text{Re}(\tilde{y}_R) - \sqrt{\sigma_T^2 \Gamma_T} \right) \tan \phi, \quad (12)$$

where the scalar  $\Gamma_T$  denotes the desired maximum SNR for the potential eavesdropper and  $\sqrt{\sigma_T^2 \Gamma_T}$  corresponds to  $\gamma_e$  in Fig. 1. As illustrated in Fig. 1, the destructive region can be divided to three zones and the inequality (12) holds when any one of the following constraints is fulfilled.

$$\text{zone 1 : } \text{Re}(\alpha_0 \tilde{\mathbf{a}}_t^H(\theta_0) \mathbf{x}) - \sqrt{\sigma_T^2 \Gamma_T} \leq 0 \quad (13a)$$

zone 2 :

$$\text{Im}(\alpha_0 \tilde{\mathbf{a}}_t^H(\theta_0) \mathbf{x}) \geq \left( \text{Re}(\alpha_0 \tilde{\mathbf{a}}_t^H(\theta_0) \mathbf{x}) - \sqrt{\sigma_T^2 \Gamma_T} \right) \tan \phi$$

$$\text{and } \text{Re}(\alpha_0 \tilde{\mathbf{a}}_t^H(\theta_0) \mathbf{x}) > \sqrt{\sigma_T^2 \Gamma_T} \quad (13b)$$

zone 3 :

$$-\text{Im}(\alpha_0 \tilde{\mathbf{a}}_t^H(\theta_0) \mathbf{x}) \geq \left( \text{Re}(\alpha_0 \tilde{\mathbf{a}}_t^H(\theta_0) \mathbf{x}) - \sqrt{\sigma_T^2 \Gamma_T} \right) \tan \phi$$

$$\text{and } \text{Re}(\alpha_0 \tilde{\mathbf{a}}_t^H(\theta_0) \mathbf{x}) > \sqrt{\sigma_T^2 \Gamma_T}. \quad (13c)$$

For simplicity, we denote (13) as destructive interference (DI) constraints. Then, we proceed to the optimization-based non-linear mapping scheme with 1-bit DACs [13] by taking the full region of destructive interference into consideration. The resulting optimization problem can be formulated as

$$\max_{\mathbf{x}} \frac{\mu |\mathbf{w}^H \mathbf{U}(\theta_0) \mathbf{x}|^2}{\mathbf{w}^H (\boldsymbol{\Sigma}(\mathbf{x}) + \mathbf{I}_{N_R}) \mathbf{w}} \quad (14a)$$

$$\text{s.t. } |x_n| \in \left\{ \pm \sqrt{\frac{P_0}{2N_T}} \pm \sqrt{\frac{P_0}{2N_T}} j \right\}, n = 1, \dots, N_T \quad (14b)$$

$$|\text{Im}(\tilde{\mathbf{h}}_k^H \mathbf{x})| \leq \left( \text{Re}(\tilde{\mathbf{h}}_k^H \mathbf{x}) - \sqrt{\sigma_{C_k}^2 \Gamma_k} \right) \tan \phi, \forall k \quad (14c)$$

$$13(a) \text{ or } 13(b) \text{ or } 13(c), \quad (14d)$$

where  $P_0$  denotes the transmit power budget.

#### B. Efficient Solver

We note that the non-convexity lies in the objective function and constraint (14b), and one can stay in the convex feasible region by exploiting various linear iteration schemes. Firstly, we convert the objective function into its linear approximation form. Following the *Dinkelbach's transform* of FP problem presented in [14], we reformulate the objective function as

$$\max_{\mathbf{x}} \mu |\mathbf{w}^H \mathbf{U}(\theta_0) \mathbf{x}|^2 - u \mathbf{w}^H (\boldsymbol{\Sigma}(\mathbf{x}) + \mathbf{I}_{N_R}) \mathbf{w} \quad (15)$$

$$\text{s.t. } 14(b), 14(c) \text{ and } 14(d).$$

Here, the objective function is still non-concave because of the first term. To proceed with optimization problem (18), let us firstly denote  $f(\mathbf{x}) = |\mathbf{w}^H \mathbf{U}(\theta_0) \mathbf{x}|^2$ . Then, we approximate the objective function  $f(\mathbf{x})$  by its first-order Taylor expansion with respect to  $\mathbf{x}$  at  $\mathbf{x}' \in \mathcal{D}$ , where  $\mathcal{D}$  denotes the feasible region of (17).

$$\begin{aligned} f(\mathbf{x}) &\approx f(\mathbf{x}') + \nabla f^H(\mathbf{x}')(\mathbf{x} - \mathbf{x}') \\ &= f(\mathbf{x}') + \\ &\quad \text{Re} \left( \left( 2 \left( \mathbf{x}'^H \mathbf{U}^H(\theta_0) \mathbf{w} \right) \mathbf{U}^H(\theta_0) \mathbf{w} \right)^H (\mathbf{x} - \mathbf{x}') \right), \end{aligned} \quad (16)$$

where  $\nabla f(\cdot)$  denotes the gradient of  $f(\cdot)$ . For simplicity, we omit the constant term  $f(\mathbf{x}')$  and denote

$$\begin{aligned} g(\mathbf{x}) &= \\ &\quad \text{Re} \left( \left( 2 \left( \mathbf{x}^{m-1}{}^H \mathbf{U}^H(\theta_0) \mathbf{w} \right) \mathbf{U}^H(\theta_0) \mathbf{w} \right)^H (\mathbf{x} - \mathbf{x}^{m-1}) \right). \end{aligned} \quad (17)$$

Herewith, the  $m$ -th iteration of the FP algorithm can be obtained by solving the following convex optimization problem

$$\begin{aligned} \max_{\mathbf{x}} \quad &\mu g(\mathbf{x}) - u \mathbf{w}^H (\boldsymbol{\Sigma}(\mathbf{x}) + \mathbf{I}_{N_R}) \mathbf{w} \\ \text{s.t.} \quad &14(b), 14(c) \text{ and } 14(d), \end{aligned} \quad (18)$$

where  $\mathbf{x}^{m-1} \in \mathcal{D}$  is the point obtained at the  $(m-1)$ -th iteration. The optimal solution  $\mathbf{x}^m \in \mathcal{D}$  can be obtained by solving problem (21), and then the receive beamformer  $\mathbf{w}^m$  can be obtained by substituting  $\mathbf{x}^m$  in (13). Furthermore,  $u$  is an auxiliary variable, which is updated iteratively by

$$u^{m+1} = \frac{\mu |\mathbf{w}^H \mathbf{U}(\theta_0) \mathbf{x}^m|^2}{\mathbf{w}^H (\boldsymbol{\Sigma}(\mathbf{x}^m) + \mathbf{I}_{N_R}) \mathbf{w}}. \quad (19)$$

It is easy to prove the convergence of the algorithm given the non-increasing property of  $u$  during each iteration [14]. With respect to the non-convex constraint lies in (14b), we then relax the strict modulus constraints on  $x_n, \forall n$  and recast the problem above as [15]

$$\max_{\hat{\mathbf{x}}} \quad \mu g(\hat{\mathbf{x}}) - u \mathbf{w}^H (\boldsymbol{\Sigma}(\hat{\mathbf{x}}) + \mathbf{I}_{N_R}) \mathbf{w} \quad (20a)$$

$$\text{s.t.} \quad |\text{Re}(\hat{x}_n)| \leq \sqrt{\frac{P_0}{2N_T}}, |\text{Im}(\hat{x}_n)| \leq \sqrt{\frac{P_0}{2N_T}}, \forall n \quad (20b)$$

$$14(c) \text{ and } 14(d). \quad (20c)$$

We note that the problem above is convex and can be solved by CVX toolbox [16]. However, the elements in the resultant waveform  $\hat{\mathbf{x}}$  cannot guarantee the strict equality for the real and imaginary part of  $\hat{x}_n$ . Thus, we normalize the optimal 1-bit DAC waveform following

$$x_n = \text{sgn}[\text{Re}(\hat{x}_n)] \sqrt{\frac{P_0}{2N_T}} + \text{sgn}[\text{Im}(\hat{x}_n)] \sqrt{\frac{P_0}{2N_T}} j, \forall n, \quad (21)$$

where  $\text{sgn}[\cdot]$  denotes the sign function.

Till now, problem (14) is converted into a convex optimization problem which includes three subproblems. By solving the problems above, we can obtain optimal waveforms  $\mathbf{x}_1^*, \mathbf{x}_2^*, \mathbf{x}_3^*$

corresponding to the aforementioned constraints (13a), (13b) and (13c), respectively. Then, we substitute each of them in the objective function, the one resulting in maximum  $\text{SINR}_{rad}$  will be the final solution to problem (14).

### C. 1-bit Quantization Constant Modulus Design

Since the extreme case of 1-bit DACs represents a special case of coarsely quantized CE signals [17], [18], we explore the 1-bit quantized CE precoding in this subsection. Herewith, the optimization problem is formulated as

$$\max_{\mathbf{x}} \quad \frac{\mu |\mathbf{w}^H \mathbf{U}(\theta_0) \mathbf{x}|^2}{\mathbf{w}^H (\boldsymbol{\Sigma}(\mathbf{x}) + \mathbf{I}_{N_R}) \mathbf{w}} \quad (22a)$$

$$\text{s.t.} \quad |x_n| = \sqrt{\frac{P_0}{N_T}}, n = 1, \dots, N_T \quad (22b)$$

$$14(c) \text{ and } 14(d). \quad (22c)$$

As the objective function in (14) has been equivalently transformed to be convex in (20), we relax CE constraints and recast the problem as

$$\max_{\tilde{\mathbf{x}}} \quad \mu g(\tilde{\mathbf{x}}) - u \mathbf{w}^H (\boldsymbol{\Sigma}(\tilde{\mathbf{x}}) + \mathbf{I}_{N_R}) \mathbf{w} \quad (23a)$$

$$\text{s.t.} \quad |\tilde{x}_n| \leq \sqrt{\frac{P_0}{N_T}}, n = 1, \dots, N_T \quad (23b)$$

$$14(c) \text{ and } 14(d). \quad (23c)$$

We note that the relaxed form above is a second-order cone program (SOCP) and can be effectively solved. In order to achieve a full CE waveform design for all the antennas at the BS we need to force the equality constrained before transmission. More specifically, we normalize the optimal waveform  $\tilde{\mathbf{x}}$  following

$$\tilde{x}_n = \begin{cases} \tilde{x}_n / \left( \sqrt{\frac{P_0}{N_T}} |\tilde{x}_n| \right) & \text{if } |\tilde{x}_n| \neq \sqrt{P_0/N_T}, \forall n \\ \tilde{x}_n & \text{if } |\tilde{x}_n| = \sqrt{P_0/N_T}, \forall n \end{cases} \quad (24)$$

We consider that phase shifters (PSs) are controlled digitally in practical applications and the weight of each PS is assumed to be a finite number of values depending on the quantization bits. Thus, when we deploy 1-bit resolution PSs, we discrete the phase of  $\tilde{x}_n, \forall n$  by (21).

## IV. NUMERICAL RESULTS

In this section, we evaluate the proposed methods via Monte Carlo based simulation results given as follows. Without loss of generality, each entry of the channel vector  $\mathbf{h}_k$  is assumed to obey standard Complex Gaussian distribution. We assume that both the DFRC BS and the radar receiver are equipped with uniform linear arrays (ULAs) with the same number of elements with half-wavelength spacing between adjacent antennas. In the following simulations, the power budget is set as  $P_0 = 30\text{dBm}$  and the Rician coefficient is given as  $v_k = 1$ . The target is located at  $\theta_0 = 0^\circ$  with a reflecting power of  $|\alpha_0|^2 = 10\text{dB}$  and clutter sources are located at  $-50^\circ, -20^\circ, 20^\circ, 50^\circ$  reflecting a power of 20dB. The SNR

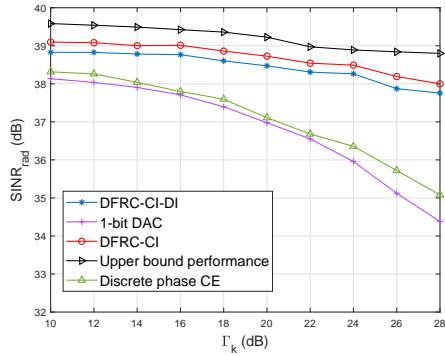


Fig. 2. The performance of radar SINR versus CU's SNR with and without hardware efficiency constraints,  $N_T = N_R = 10$ ,  $K = 5$ .

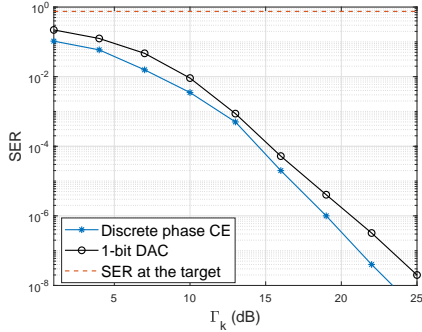


Fig. 3. SER of CU versus SNR threshold  $\Gamma_k$  when target location is known precisely,  $N_T = N_R = 10$ ,  $K = 5$ .

threshold  $\Gamma_T$  is set as  $-1$  dB as default unless it is presented specifically.

The tradeoff between the given SNR threshold of CUs and the radar receive SINR is illustrated in Fig. 2, where the hardware-efficient constraints are deployed and not deployed. We note that the hardware-efficient designs, i.e., both the discrete phase CE and 1-bit DACs approaches, deteriorate the performance of radar SINR. Furthermore, the 1-bit quantized CE outperforms the 1-bit DAC technique, which is for the reason that the feasible region of problem (22) is larger than that of problem (14). In Fig. 3, the average SER of CUs versus threshold SNR  $\Gamma_k$  is depicted, where the red dashed line demonstrates the SER at the target. It is noted that the SER at the target is much higher than CUs, which indicates the proposed algorithm ensures the system security effectively.

## V. CONCLUSION

In this paper, we have formulated and solved hardware-efficient optimization problems for secure DFRC systems based on CI technique. Specifically, 1-bit DACs and the discrete phase CE method have been taken into consideration for reducing the hardware cost. The numerical results have proved the effectiveness of CI-based security design. Moreover, the deployment of the 1-bit quantized CE constraints followed by a normalization method has achieved higher radar receive SINR comparing with 1-bit DACs.

## ACKNOWLEDGMENT

This work has received funding from the Engineering and Physical Sciences Research Council (EPSRC) of the UK Grant number EP/S026622/1, the UK MOD University Defence Research Collaboration (UDRC) in Signal Processing and the China Scholarship Council (CSC).

## REFERENCES

- [1] M. R. Khandaker, C. Masouros, K.-K. Wong, and S. Timotheou, "Secure SWIPT by exploiting constructive interference and artificial noise," *IEEE Transactions on Communications*, vol. 67, no. 2, pp. 1326–1340, 2018.
- [2] M. R. Khandaker, C. Masouros, and K.-K. Wong, "Constructive interference based secure precoding: A new dimension in physical layer security," *IEEE Transactions on Information Forensics and Security*, vol. 13, no. 9, pp. 2256–2268, 2018.
- [3] Z. Wei and C. Masouros, "Device-Centric distributed antenna transmission: Secure precoding and antenna selection with interference exploitation," *IEEE Internet of Things Journal*, vol. 7, no. 3, pp. 2293–2308, 2020.
- [4] Z. Wei, C. Masouros, and F. Liu, "Secure directional modulation with Few-Bit phase shifters: Optimal and Iterative-Closed-Form designs," *IEEE Transactions on Communications*, 2020.
- [5] A. Li, C. Masouros, X. Liao, Y. Li, and B. Vucetic, "Multiplexing more data streams in the MU-MISO downlink by interference exploitation precoding," in *2020 IEEE Wireless Communications and Networking Conference (WCNC)*. IEEE, 2020, pp. 1–6.
- [6] S. Zhang, R. Zhang, and T. J. Lim, "Constant envelope precoding for MIMO systems," *IEEE Transactions on Communications*, vol. 66, no. 1, pp. 149–162, 2017.
- [7] M. Kazemi, H. Aghaeinia, and T. M. Duman, "Discrete-phase constant envelope precoding for massive MIMO systems," *IEEE Transactions on Communications*, vol. 65, no. 5, pp. 2011–2021, 2017.
- [8] X. Hu, C. Zhong, X. Chen, W. Xu, and Z. Zhang, "Cluster grouping and power control for angle-domain MmWave MIMO NOMA systems," *IEEE Journal of Selected Topics in Signal Processing*, vol. 13, no. 5, pp. 1167–1180, 2019.
- [9] L. Zhao, G. Geraci, T. Yang, D. W. K. Ng, and J. Yuan, "A tone-based AoA estimation and multiuser precoding for millimeter wave massive MIMO," *IEEE Transactions on Communications*, vol. 65, no. 12, pp. 5209–5225, 2017.
- [10] C. Masouros and G. Zheng, "Exploiting known interference as green signal power for downlink beamforming optimization," *IEEE Transactions on Signal processing*, vol. 63, no. 14, pp. 3628–3640, 2015.
- [11] Q. Xu, P. Ren, and A. L. Swindlehurst, "Rethinking secure precoding via interference exploitation: A smart eavesdropper perspective," *IEEE Transactions on Information Forensics and Security*, vol. 16, pp. 585–600, 2020.
- [12] A. Kalantari, M. Soltanalian, S. Maleki, S. Chatzinotas, and B. Ottersten, "Directional modulation via symbol-level precoding: A way to enhance security," *IEEE Journal of Selected Topics in Signal Processing*, vol. 10, no. 8, pp. 1478–1493, 2016.
- [13] A. Li, C. Masouros, F. Liu, and A. L. Swindlehurst, "Massive MIMO 1-bit DAC transmission: A low-complexity symbol scaling approach," *IEEE Transactions on Wireless Communications*, vol. 17, no. 11, pp. 7559–7575, 2018.
- [14] K. Shen and W. Yu, "Fractional programming for communication systems part I: Power control and beamforming," *IEEE Transactions on Signal Processing*, vol. 66, no. 10, pp. 2616–2630, 2018.
- [15] P. V. Amadori and C. Masouros, "Constant envelope precoding by interference exploitation in phase shift keying-modulated multiuser transmission," *IEEE Transactions on Wireless Communications*, vol. 16, no. 1, pp. 538–550, 2016.
- [16] S. Boyd, S. P. Boyd, and L. Vandenberghe, *Convex optimization*. Cambridge university press, 2004.
- [17] A. Mezghani, R. Ghiat, and J. A. Nossek, "Transmit processing with low resolution D/A-converters," in *2009 16th IEEE International Conference on Electronics, Circuits and Systems-ICECS 2009*. IEEE, 2009, pp. 683–686.
- [18] H. Jedda, A. Mezghani, A. L. Swindlehurst, and J. A. Nossek, "Quantized constant envelope precoding with PSK and QAM signaling," *IEEE Transactions on Wireless Communications*, vol. 17, no. 12, pp. 8022–8034, 2018.